Journal of Peptide Science
J. Pept. Sci. 2007; **13**: 190–205
Published online 17 January 2007 in Wiley InterScience (www.interscience.wiley.com). DOI: 10.1002/psc.833

JOURNAL OF PEPTIDE SCIENCE

Crystal-state 3D-structural characterization of novel, Aib-based, turn and helical peptides

MARCO CRISMA,* ERIKA ANDREETTO, MARTA DE ZOTTI, ALESSANDRO MORETTO, CRISTINA PEGGION, FERNANDO FORMAGGIO and CLAUDIO TONIOLO

Institute of Biomolecular Chemistry, CNR, Department of Chemistry, University of Padova, 35131 Padova, Italy

Received 20 November 2006; Accepted 2 December 2006

Abstract: The crystal-state conformations of the hexapeptide amide Pht-(Aib)$_6$-NH-C(CH$_3$)$_2$-*O*-O*t*Bu (7), the hexapeptide Ac-L-*a*Ile-(Aib)$_5$-O*t*Bu (6), the pentapeptide Z-(Aib)$_3$-L-Glu(O*t*Bu)-Aib-*O*-(CH$_2$)$_2$-(1)Nap (5), the tetrapeptides Z-(Aib)$_2$-L-His(N$^\tau$-Trt)-Aib-OMe (4 I) and Z-(Aib)$_2$-L-Nva-Aib-O*t*Bu (4 II), the tripeptide Pyr-(Aib)$_3$-O*t*Bu (3 I), the dipeptide amides Pyr-(Aib)$_2$-(4)NH-TEMPO (3 II) and Piv-(Aib)$_2$-NH-C(CH$_3$)$_2$-*O*-O*t*Bu (3 III), and the dipeptides Pht-Aib-βAc$_6$c-O*t*Bu (2 I), Pht-Aib-NH-C(CH$_3$)$_2$-*O*-O*t*Bu (2 II) and Boc-*g*Gly-*m*Aib-OH (2 III) have been determined by X-ray diffraction analyses. All peptides investigated are characterized by one or more turn/helix forming Aib residues. Except the three short dipeptides, all are folded into C=O···H–N intramolecularly H-bonded 3$_{10}$-helices, or into various types of β-turns. In the structure of 6, two independent molecules of opposite screw sense were observed in the asymmetric unit, generating diastereomeric 3$_{10}$-helices. Copyright © 2007 European Peptide Society and John Wiley & Sons, Ltd.

Keywords: α-aminoisobutyric acid; crystal-state structures; 3$_{10}$-helix; x-ray diffraction; β-turn

INTRODUCTION

Aib (α-aminoisobutyric acid or C$^{\alpha,\alpha}$-dimethylglycine) is the simplest achiral member of the family of C$^\alpha$-tetrasubstituted α-amino acids [1–4]. Pioneering theoretical conformational studies on Ac-Aib-NHMe (Ac, acetyl; NHMe, methylamino) showed that the presence of two methyl groups on the C$^\alpha$-atom (Thorpe-Ingold effect) imposes a marked restriction on the available ϕ,ψ space [5–8]. Type III/III′ β-turns [9–11] and helical structures of the 3$_{10}$ – or the α-helical type [12–18] are significantly populated as opposed to more extended structures. Conversely, the energy difference and barrier between the 3$_{10}$- and α-helices are small. While Aib may accommodate in position i + 2 either type I/I′ or type II/II′; β-turns and γ-turns [10,19], *semi*-extended and fully extended (C$_5$) [10,20,21] structures are extremely unusual for this residue. Aib peptides do not tend to form β-sheet structures, and, in general, their propensity to give strongly self-associated species is low. For the same reason, Aib proved to be the best β-sheet breaker α-amino acid [22]. This property was helpful in designing β-sheet inhibitors as drug candidates for conformational diseases [23,24].

The extremely strong propensity of Aib-based peptides to form single crystals allowed detailed X-ray diffraction analyses to be performed on a very high number of compounds. The histogram in Figure 1 clearly shows the remarkable percentage (18.7%) of X-ray diffraction structures of Aib-containing peptides published from 1973 to 2004 (a total of 305 structures) as compared to those of peptides not containing any C$^\alpha$-tetrasubstituted α-amino acid (a total of 1631).

In this paper, the crystal-state 3D-structural characterization by X-ray diffraction of eleven peptides, eight of which are long enough to form at least a single β-turn, is presented. All peptides investigated are heavily based on the Aib residue. Their primary structures are as follows:

(i) Pht-(Aib)$_6$-NH-C(CH$_3$)$_2$-O-O*t*Bu (**7**)
(ii) Ac-L-*a*Ile-(Aib)$_5$-O*t*Bu (**6**)
(iii) Z-(Aib)$_3$-L-Glu(O*t*Bu)-Aib-*O*-(CH$_2$)$_2$-(1)Nap (**5**)
(iv) Z-(Aib)$_2$-L-His(N$^\tau$-Trt)-Aib-OMe (**4 I**)
(v) Z-(Aib)$_2$-L-Nva-Aib-O*t*Bu (**4 II**)
(vi) Pyr-(Aib)$_3$-O*t*Bu (**3 I**)
(vii) Pyr-(Aib)$_2$-(4)NH-TEMPO (**3 II**)
(viii) Piv-(Aib)$_2$-NH-C(CH$_3$)$_2$-*O*-O*t*Bu (**3 III**)
(ix) Pht-Aib-βAc$_6$c-O*t*Bu (**2 I**)
(x) Pht-Aib-NH-C(CH$_3$)$_2$-*O*-O*t*Bu (**2 II**)
(xi) and Boc-*g*Gly-*m*Aib-OH (**2 III**)

[Z, benzyloxycarbonyl; OMe, methoxy; Pht, phthaloyl; O*t*Bu, *tert*-butoxy; Nap, naphthyl; Trt, trityl or triphenylmethyl; Pyr, 1-pyrenecarbonyl; TEMPO, 2,2,6,6-tetramethylpiperidine-1-oxyl; Piv, pivaloyl or *tert*-butylcarbonyl; βAc$_6$c, *trans-rac*-2-aminocyclohexanecarbonyl; *g*Gly, 'geminal Gly'; *m*Aib, 'malonyl Aib'. The arabic numbers designate the number of amino groups present in the molecule].

*Correspondence to: M. Crisma, Institute of Biomolecular Chemistry, CNR, Department of Chemistry, University of Padova, via Marzolo 1, 35131 Padova, Italy; e-mail: marco.crisma@unipd.it

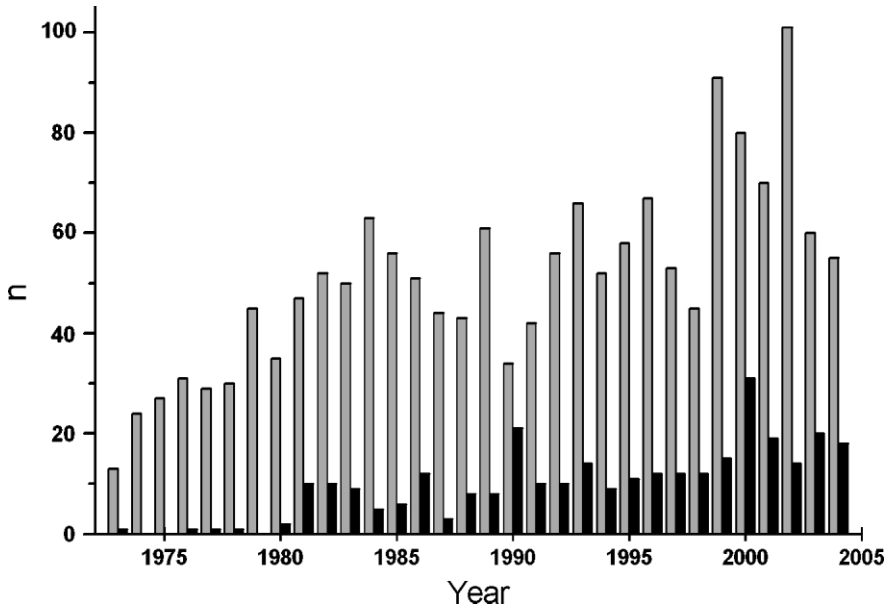

Figure 1 Histogram showing the number of X-ray diffraction structures of Aib-containing peptides (black bars) deposited at the Cambridge Structural Database from 1973 to 2004 as compared to all those not containing any C^{α}-tetrasubstituted α-amino acid (gray bars).

Table 1 Physical Properties and Analytical Data for the Newly Synthesized Peptides Studied in this Work

Peptide	Recryst. solvent[a]	Mp (°C)	$[\alpha]_D^{20}$[b]	TLC			IR (cm^{-1})
				R_f1	R_f2	R_f3	
Ac-L-*a*Ile-$(Aib)_5$-O*t*Bu (**6**)	EtOAc/PE	225–227	−2.2	0.70	0.95	0.45	3317, 1734, 1662, 1533
Z-$(Aib)_3$-L-Glu(O*t*Bu)-Aib-*O*-$(CH_2)_2$-(1)Nap (**5**)	MeCN	190–191	−10.2	0.80	0.95	0.60	3307, 1734, 1704, 1668, 1650, 1540
Z-$(Aib)_2$-L-His(N^{τ}-Trt)-Aib-Ome (**4 I**)	EtOAc	205–207	−6.1	0.70	0.90	0.35	3344, 1739, 1681, 1659, 1530
Z-$(Aib)_2$-L-Nva-Aib-O*t*Bu (**4 II**)	EtOAc/PE	166–167	−8.1	0.75	0.90	0.25	3341, 1731, 1708, 1655, 1528
Pyr-$(Aib)_3$-O*t*Bu (**3 I**)	CH_2Cl_2/PE	200–202	—	0.60	0.95	0.25	3412, 3335, 1735, 1668, 1650, 1534
Pyr-$(Aib)_2$-(4)NH-TEMPO (**3 II**)	EtOAc/PE	232–233	—	0.55	0.90	0.10	3392, 1687, 1637, 1547
Piv-$(Aib)_2$-NH-$C(CH_3)_2$-*O*-O*t*Bu (**3 III**)	EtOAc/PE	147–148	—	0.75	0.50	0.20	3384, 3340, 1671, 1537
Pht-Aib-βAc_6c-O*t*Bu (**2 I**)	EtOAc/PE	152–154	—	0.90	0.90	0.55	3353, 1775, 1716, 1701, 1677, 1528

[a] EtOAc, ethyl acetate; PE, petroleum ether; MeCN, acetonitrile.
[b] c = 0.5 (methanol).

MATERIALS AND METHODS

Synthesis and Characterization of Peptides

Melting points were determined using a Leitz (Wetzlar, Germany) model Laborlux 12 apparatus and are not corrected. Optical rotations were measured using a Perkin-Elmer (Norwalk, CT, USA) model 241 polarimeter equipped with a Haake (Karlsruhe, Germany) model D thermostat. Thin-layer chromatography was performed on Merck (Darmstadt, Germany) Kieselgel $60F_{254}$ precoated plates using the following solvent systems: 1 ($CHCl_3$–ethanol 9 : 1), 2 (1-butanol–acetic acid–water 3 : 1 : 1), 3 (toluene–ethanol 7 : 1). The chromatograms were examined by UV fluorescence or developed by chlorine–starch–potassium iodide or ninhydrin chromatic reaction as appropriate. All compounds were obtained in a chromatographically homogeneous state. The solid-state IR absorption spectra were recorded with a Perkin–Elmer model 1720X FT-IR spectrophotometer. The ^{1}H-NMR spectra were recorded with a Bruker (Karlsruhe, Germany) model AM 400 spectrometer. Measurements were carried out in deuterochloroform (99.96% d; Aldrich, Milwaukee, WI, USA) with tetramethylsilane as the internal standard. The physical properties and analytical data for the newly synthesized peptides are listed in Table 1. All compounds were also characterized by ^{1}H-NMR spectrometry (data not shown). The syntheses and characterizations of peptides **2 II** [25], **2 III** [26], and **7** [25] have already been reported.

DOI: 10.1002/psc

X-Ray Diffraction

Single crystals of peptides **7**-**2 III** were grown from the solvents shown in Tables 2 and 3. Intensity data collections were performed using a Philips PW1100 four-circle diffractometer in the $\theta/2\theta$ scan mode. For **4 I** data were collected with graphite-monochromated MoKα radiation ($\lambda = 0.71073$ Å). In all other instances graphite-monochromated CuKα radiation ($\lambda = 1.54178$ Å) was employed. Cell parameters were obtained by least-squares refinements of the angular settings of 48 carefully centered, high-angle reflections. Intensities were corrected for Lorentz and polarization effects, not for absorption. The structures were solved by direct methods, using the SHELXS 86 [27], SHELXS 97 [28], or the SIR 2002 [29] program (Tables 2 and 3). Refinements were carried out by least-squares procedures on F^2, using all data, by application of the SHELXL 93 [30] or the SHELXL 97 [31] program, with all nonH atoms anisotropic. H-atoms of all peptide molecules were calculated at idealized positions and refined using a riding model. Details specific to each individual structure are given below.

In **7**, disorder was found at the level of the *C*-terminal -C(CH_3)$_2$-*O*-O*t*Bu moiety. Its two oxygen atoms were refined on two sets of positions (atoms OT1, OT2, and OT1′, OT2′), each with a population parameter of 0.50. Restraints were imposed upon the anisotropic displacement parameters of the disordered atoms.

The occurrence of two, conformationally distinct, independent peptide molecules characterizes the structure of **6**.

The asymmetric unit of **5** is composed of 4 independent peptide molecules for a total of 240 nonH atoms. In addition to the large number of atoms, structure solution was further complicated by the weak diffracting power shown by the crystal which, in turn, might be ascribed to the crystal thickness (lowest dimension $\cong 0.05$ mm). Indeed, only 25 and 11% of the collected reflections had $I \geq 2\sigma(I)$ in the 1.2–1.1 Å and the 1.1–1.0 Å resolution ranges, respectively. The structure was eventually solved by the SIR2002 program in its default mode for large structures by using 2687 E-values >1.2. Among 200 trials, that with the best figure of merit allowed the location of 107 atoms in three well recognizable peptide fragments. These atoms were used as input in the SHELXS 97 program for the structure expansion with the tangent formula using 4401 E-values > 0.9, which allowed the location of 47 additional atoms. The positions of the remaining atoms, mostly belonging to the Glu(O*t*Bu) side chains and the *C*-terminal ethylnaphthyl ester groups of the four peptide molecules, were recovered from subsequent different Fourier maps. All phenyl and naphthyl rings were constrained to the idealized geometry. Restraints were applied to most of the bond distances, as well as to

Table 2 Crystallogaphic Data for the Longest Five Peptides Studied in this Work

	7	**6**	**5**	**4 I**	**4 II**
Empirical formula	C_{39} H_{61} N_7 O_{10}	C_{32} H_{58} N_6 O_8	C_{45} H_{61} N_5 O_{10}	C_{46} H_{52} N_6 O_7	C_{29} H_{46} N_4 O_7
Formula weight (a.m.u.)	788.0	654.8	832.0	800.9	562.7
Crystal system	Monoclinic	Triclinic	Triclinic	Monoclinic	Orthorhombic
Space group	$P2_1/n$	P1	P1	$P2_1$	$P2_12_12_1$
a (Å)	9.081(3)	9.121(2)	11.318(2)	9.686(2)	10.646(2)
b (Å)	22.300(5)	11.801(2)	16.574(3)	24.207(3)	15.696(3)
c (Å)	24.099(5)	19.145(3)	25.266(4)	10.218(2)	19.262(4)
α (°)	90	103.86(3)	85.29(6)	90	90
β (°)	98.09(9)	102.24(4)	89.57(7)	116.2(1)	90
γ (°)	90	96.46(5)	88.04(7)	90	90
V (Å^3)	4832(2)	1926.1(6)	4720.7(14)	2149.7(7)	3218.7(11)
Z (molecules/unit cell)	4	2	4	2	4
Density (calc.) (g/cm^3)	1.083	1.129	1.171	1.237	1.161
Independent reflections	7105 [*R*(int) = 0.063]	5711	9688	5295 [*R*(int) = 0.062]	2710 [*R*(int) = 0.010]
Observed reflections	5303 [$I \geq 2\sigma(I)$]	5144 [$I \geq 2\sigma(I)$]	4181 [$I \geq 2\sigma(I)$]	1826 [$I \geq 2\sigma(I)$]	1724 [$I \geq 2\sigma(I)$]
Solved by	SIR2002	SIR2002	SIR2002	SHELXS 86	SHELXS 97
Refined by	SHELXL 97	SHELXL 97	SHELXL 97	SHELXL 93	SHELXL 97
S	1.286	1.087	0.897	0.815	0.902
Final *R* indices [$I \geq 2\sigma(I)$]	$R_1 = 0.100$ $wR_2 = 0.302$	$R_1 = 0.049$ $wR_2 = 0.146$	$R_1 = 0.086$ $wR_2 = 0.202$	$R_1 = 0.054$ $wR_2 = 0.126$	$R_1 = 0.038$ $wR_2 = 0.081$
R indices (all data)	$R_1 = 0.115$ $wR_2 = 0.312$	$R_1 = 0.053$ $wR_2 = 0.154$	$R_1 = 0.170$ $wR_2 = 0.243$	$R_1 = 0.206$ $wR_2 = 0.176$	$R_1 = 0.076$ $wR_2 = 0.093$
Temperature (K)	293(2)	293(2)	293(2)	293(2)	293(2)
Radiation (λ, Å)	CuKα (1.54178)	CuKα (1.54178)	CuKα (1.54178)	MoKα (0.71073)	CuKα (1.54178)
Crystallization solvent	EtOAc[a]/PE[a]	EtOAc/PE	EtOH[a]	MeOH[a]	EtOAc/PE
Crystal size (mm)	0.50 × 0.50 × 0.35	0.35 × 0.35 × 0.25	0.45 × 0.20 × 0.05	0.40 × 0.20 × 0.14	0.30 × 0.20 × 0.15
$\Delta\rho_{max}$ and $\Delta\rho_{min}$ (e•Å^{-3})	0.502/−0.260	0.338/−0.169	0.354/−0.385	0.191/−0.236	0.150/−0.145

[a] EtOAc, ethyl acetate; PE, petroleum ether; EtOH, ethanol; MeOH, methanol.

DOI: 10.1002/psc

Table 3 Crystallogaphic Data for the Additional Six Peptides Studied in this Work

	3 I	**3 II**	**3 III**	**2 I**	**2 II**	**2 III**
Empirical formula	C_{33} H_{39} N_3O_5	C_{34} H_{41} N_4O_4	C_{20} H_{39} N_3O_5	C_{23} H_{30} N_2O_5	C_{19} H_{26} N_2O_5	C_{11} H_{20} N_2O_5
Formula weight (a.m.u.)	557.7	569.7	401.5	414.5	362.4	260.3
Crystal system	Monoclinic	Triclinic	Orthorhombic	Monoclinic	Monoclinic	Monoclinic
Space group	$P2_1$	P-1	$P2_12_12$	$P2_1/n$	I2/a (No. 15)	$P2_1/a$
a (Å)	9.273(2)	8.912(2)	24.139(5)	10.034(3)	11.923(2)	10.073(2)
b (Å)	10.605(2)	10.657(2)	11.425(2)	18.196(3)	21.943(4)	11.957(2)
c (Å)	16.003(3)	18.262(3)	8.999(2)	12.339(3)	15.802(3)	12.914(3)
α (°)	90	91.95(7)	90	90	90	90
β (°)	105.99(7)	97.71(6)	90	99.37(7)	102.79(4)	110.12(5)
γ (°)	90	112.78(7)	90	90	90	90
V (Å^3)	1512.8(5)	1577.7(5)	2481.8(9)	2222.8(9)	4031.6(13)	1460.5(5)
Z (molecules/unit cell)	2	2	4	4	8	4
Density (calc.) (g/cm^3)	1.224	1.199	1.075	1.239	1.194	1.184
Independent reflections	2646 [R(int) = 0.075]	4660	1750 [R(int) = 0.060]	3330 [R(int) = 0.077]	2995 [R(int) = 0.027]	2166 [R(int) = 0.017]
Observed reflections	1610 [$I \geq 2\sigma(I)$]	3220 [$I \geq 2\sigma(I)$]	1197 [$I \geq 2\sigma(I)$]	2895 [$I \geq 2\sigma(I)$]	2443 [$I \geq 2\sigma(I)$]	2011 [$I \geq 2\sigma(I)$]
Solved by	SIR2002	SIR2002	SIR2002	SIR2002	SHELXS 97	SIR2002
Refined by	SHELXL 97	SHELXL 97	SHELXL 97	SHELXL 97	SHELXL 97	SHELXL 97
S	1.006	1.058	1.052	1.049	1.079	1.054
Final R indices [$I \geq 2\sigma(I)$]	$R_1 = 0.064$ $wR_2 = 0.184$	$R_1 = 0.079$ $wR_2 = 0.222$	$R_1 = 0.078$ $wR_2 = 0.220$	$R_1 = 0.054$ $wR_2 = 0.149$	$R_1 = 0.044$ $wR_2 = 0.129$	$R_1 = 0.056$ $wR_2 = 0.162$
R indices (all data)	$R_1 = 0.101$ $wR_2 = 0.213$	$R_1 = 0.103$ $wR_2 = 0.249$	$R_1 = 0.112$ $wR_2 = 0.250$	$R_1 = 0.058$ $wR_2 = 0.152$	$R_1 = 0.053$ $wR_2 = 0.134$	$R_1 = 0.058$ $wR_2 = 0.166$
Temperature (K)	293(2)	293(2)	293(2)	293(2)	293(2)	293(2)
Radiation (λ, Å)	CuKα (1.54178)	CuKα (1.54178)	CuKα (1.54178)	CuKα (1.54178)	CuKα (1.54178)	CuKα (1.54178)
Crystallization solvent	EtOAc[a] /PE[a]	EtOAc/CH_2Cl_2	EtOAc/PE	EtOAc/PE	EtOAc	MeOH[a]
Crystal size (mm)	0.30 × 0.10 × 0.05	0.40 × 0.25 × 0.15	0.50 × 0.25 × 0.10	0.50 × 0.45 × 0.40	0.40 × 0.30 × 0.25	0.60 × 0.40 × 0.40
$\Delta\rho_{max}$ and $\Delta\rho_{min}$ (e•Å^{-3})	0.219/−0.218	0.374/−0.298	0.425/−0.249	0.208/−0.272	0.290/−0.149	0.281/−0.244

[a] EtOAc, ethyl acetate; PE, petroleum ether; MeOH, methanol.

DOI: 10.1002/psc

the anisotropic displacement parameters of the nonH atoms belonging to the OtBu side-chain protecting groups and to the *C*-terminal ethylnaphthyl ester groups, to approach isotropic behavior.

In the refinement of **4 I**, the phenyl rings of the benzyloxycarbonyl and trityl groups were constrained to the idealized geometry. In the refinement of **3 III**, restraints were imposed upon the bond distances and anisotropic displacement parameters involving atoms of the *N*- and *C*-terminal groups.

It is worth pointing out that **3 I** and **3 III**, although lacking chiral centers, crystallize in noncentrosymmetric space groups. The chosen enantiomorphs are those giving the lowest Flack parameter. However, in the absence of significant anomalous scatterers, this choice does not imply any claim on the absolute structure.

CCDC 627 521–627 531 contain the supplementary crystallographic data for the structures **7**–**2 III** reported in this paper. These data can be obtained free of charge at www.ccdc.cam.ac.uk/data_request/cif [or from the Cambridge Crystallographic Data Centre, 12 Union Road, Cambridge CB2 1EZ, UK; Fax: (+44)-(0)1223-336-033; E-mail: deposit@ccdc.cam.ac.uk].

Statistical Analysis

Data on the occurrence of Aib-containing peptide crystal structures, as compared to all those not containing any C^{α}-tetrasubstituted α-amino acid, were retrieved from the Cambridge Structural Database ver. 5.27, release of November 2005 [32]. Neither simple amino acid derivatives, nor metal-organic compounds were included.

RESULTS AND DISCUSSION

The molecular and crystal structures of the eleven peptides Pht-$(Aib)_6$-NH-$C(CH_3)_2$-*O*-O*t*Bu (**7**), Ac-L-*a*Ile-$(Aib)_5$-O*t*Bu (**6**), Z-$(Aib)_3$-L-Glu(O*t*Bu)-Aib-*O*-$(CH_2)_2$-(1)Nap (**5**), Z-$(Aib)_2$-L-His(N^{τ}-Trt)-Aib-OMe (**4 I**), Z-$(Aib)_2$-L-Nva-Aib-O*t*Bu (**4 II**), Pyr-$(Aib)_3$-O*t*Bu (**3 I**), Pyr-$(Aib)_2$-(4)NH-TEMPO (**3 II**), Piv-$(Aib)_2$-NH-$C(CH_3)_2$-*O*-O*t*Bu (**3 III**), Pht-Aib-βAc_6c-O*t*Bu (**2 I**), Pht-Aib-NH-$C(CH_3)_2$-*O*-O*t*Bu (**2 II**), and Boc-*g*Gly-*m*Aib-OH (**2 III**) were elucidated by X-ray diffraction. The molecular structures are illustrated in Figures 2–12. N^{α}-Blocking groups and backbone torsion angles [33] are given in Tables 4 and 5. In Table 6 the intra- and intermolecular H-bond parameters are reported.

Bond lengths and bond angles are in general agreement with previously reported values for the geometry of the benzyloxycarbonyl [34], *tert*-butyloxycarbonyl [35], phthaloyl [36], and pivaloyl [37,38] moieties, the amide [39] and ester [40] groups, the peptide unit [41,42], and the Aib [43–45] residue.

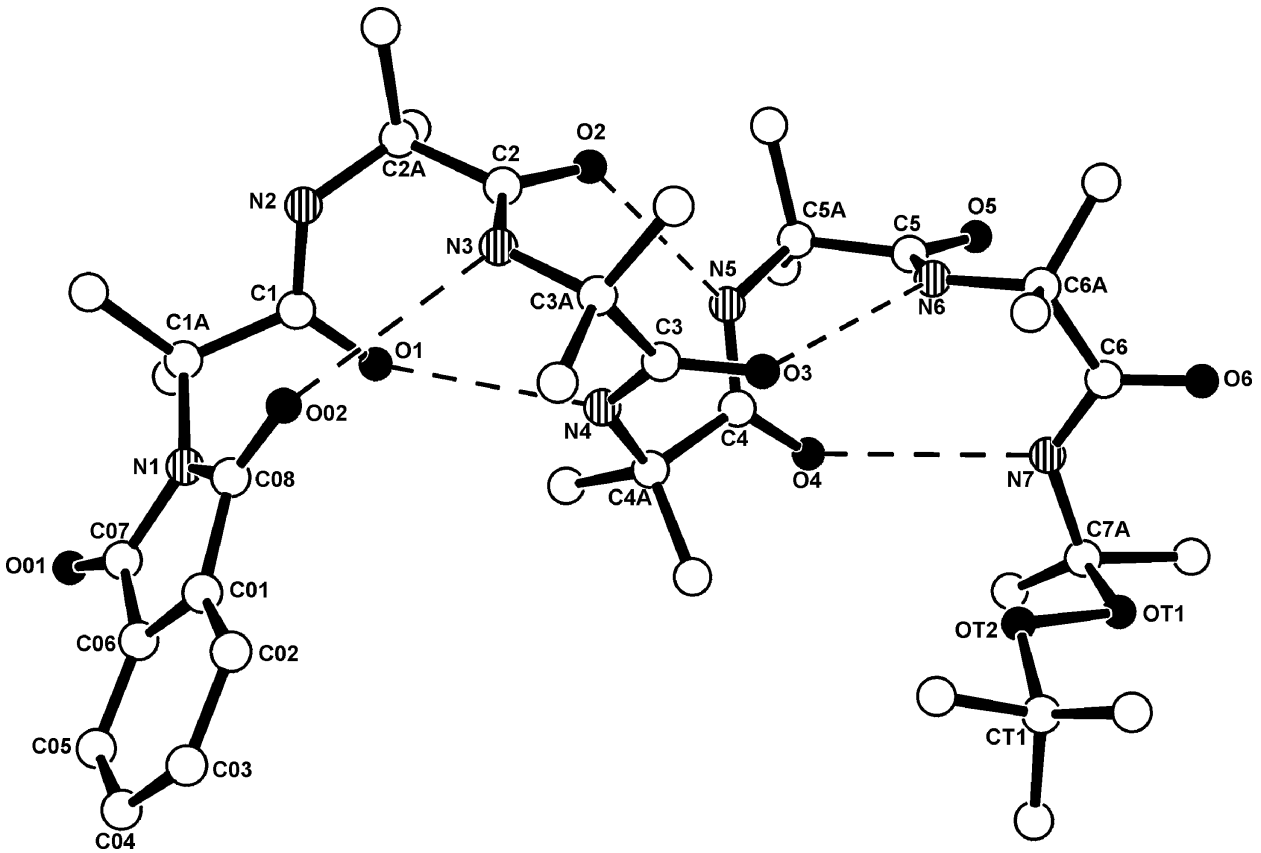

Figure 2 X-ray diffraction structure of Pht-$(Aib)_6$-NH-$C(CH_3)_2$-*O*-O*t*Bu (**7**) with numbering of the atoms. The five intramolecular H-bonds are represented by dashed lines. The second conformer of the disordered, *C*-terminal, -*O*-O*t*Bu moiety is omitted for clarity. Only the right-handed helical structure is shown.

DOI: 10.1002/psc

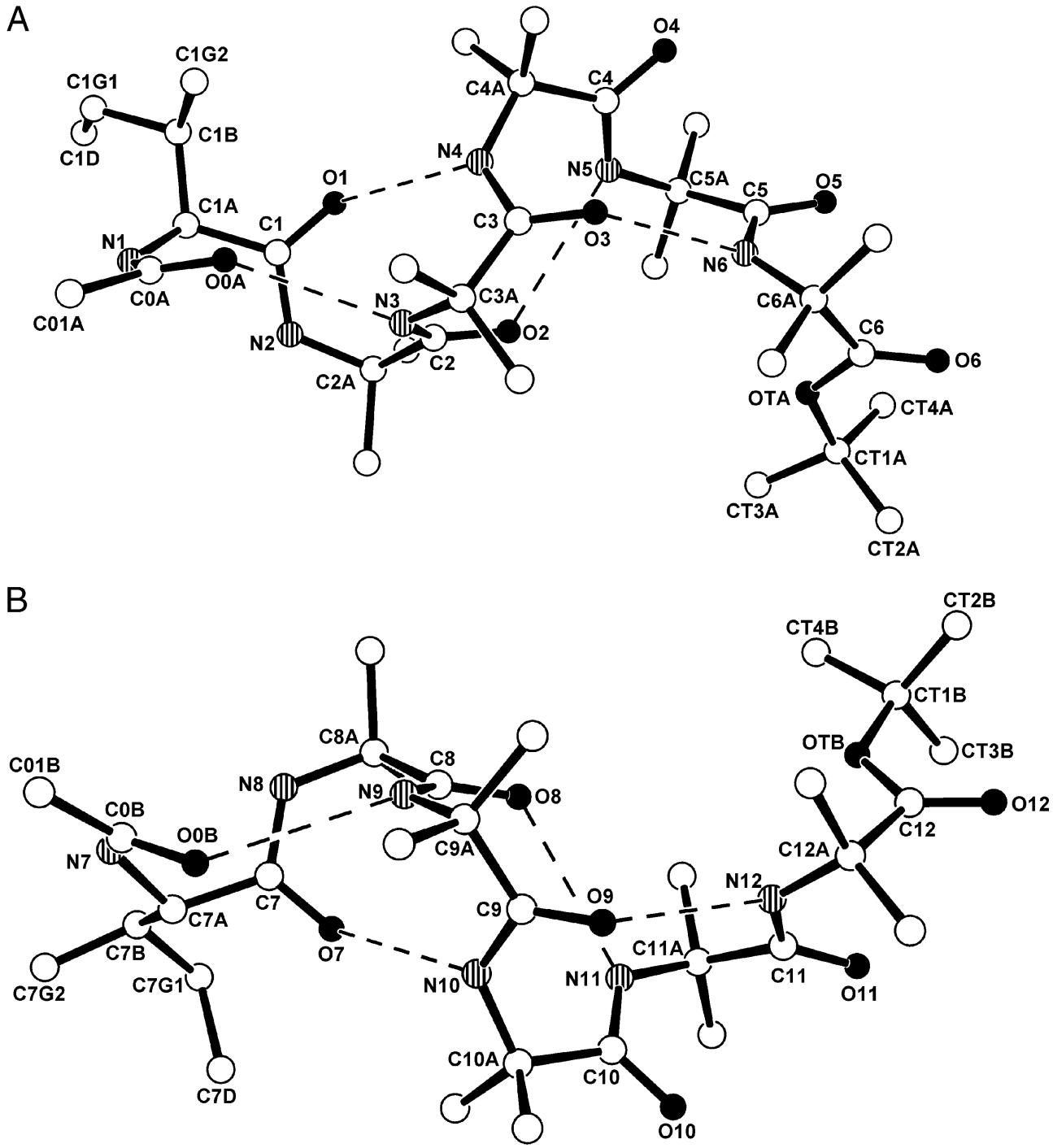

Figure 3 X-ray diffraction structures of the two independent molecules (**A** and **B**) in the asymmetric unit of Ac-L-*a*Ile-$(Aib)_5$-O*t*Bu (**6**) with numbering of the atoms. In each structure the four intramolecular H-bonds are represented by dashed lines.

The N^{α}-protected hexapeptide amide **7** adopts a folded conformation stabilized by five, consecutive C=O···H–N intramolecular H-bonds. Specifically, the sequence 1–2 is folded in a nonhelical type-II′ β-turn characterized by the *semi*-extended Aib[1] and right-handed helical Aib[2], in which one of the two carbonyl oxygens of the phthaloyl N^{α}-blocking group acts as the H-bond acceptor. This bent portion of the sequence is followed by a right-handed 3_{10}-helical structure encompassing the Aib^2–Aib^6 sequence and characterized by four consecutive C=O···H–N intramolecularly H-bonded type-III β-turns. The C=O···H–N H-bonds are of normal strength for this type of interactions [46–48].

The backbone of the two molecules (**A** and **B**) in the asymmetric unit of the N^{α}-acetylated hexapeptide ester **6** is very similar, except for the handedness which is opposite (left-handed for molecule **A** and

DOI: 10.1002/psc

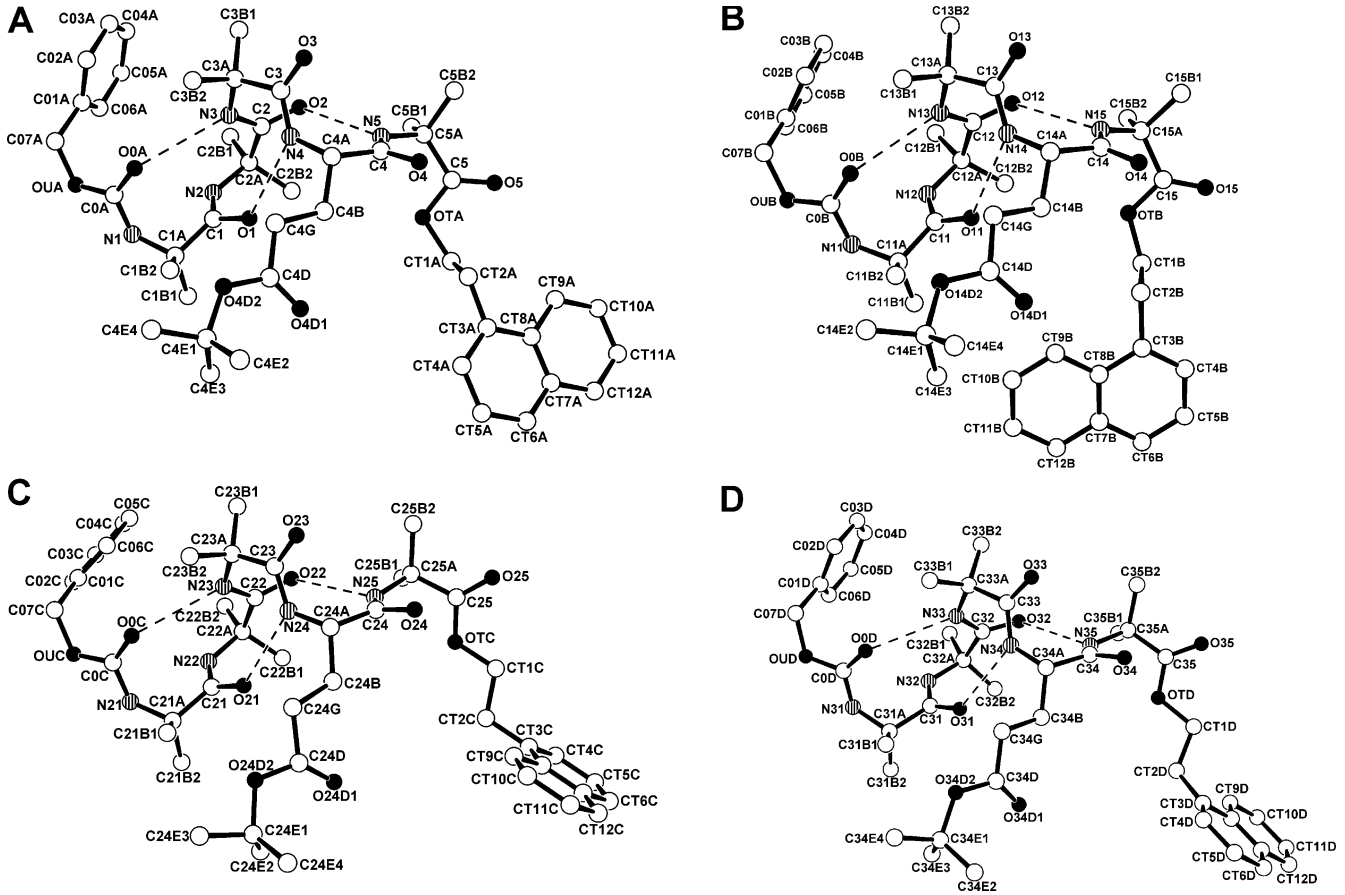

Figure 4 X-ray diffraction structures of the four independent molecules (**A**–**D**) in the asymmetric unit of Z-(Aib)$_3$-L-Glu(O*t*Bu)-Aib-*O*-(CH$_2$)$_2$-Nap (**5**). In each structure the three intramolecular H-bonds are represented by dashed lines.

right-handed for molecule **B**). The observed 3_{10}-helices are regular from residue 1 to 5 (with the single exception of residue 1 of molecule **A**). The average ϕ,ψ torsion angles are 57.0°, 35.7° (residues 2–5 of molecule **A**) and −57.3°, −37.0° (residues 1–5 of molecule **B**). These angles should be compared with those of a classical peptide 3_{10}-helix (±57°, ±30°) [13]. Also the *C*-terminal Aib residue adopts a helical conformation, but it has a handedness opposite to that exhibited by the preceding residues. This observation is quite common for 3_{10}-helical peptide esters [2–4]. Four, consecutive C=O···H–N intramolecular H-bonds stabilize the helical structure of each molecule. The occurrence of two diastereomeric helical molecules in an Aib-rich peptide containing a single chiral residue at the *N*-terminus is not an unprecedented finding [49].

All four independent molecules (**A**–**D**) in the asymmetric unit of the fully protected pentapeptide ester **5** are right-handed 3_{10}-helical, characterized by three, consecutive, C=O···H–N intramolecular H-bonds. The four sets of ϕ,ψ torsion angles are close to each other and regular, except those of residue 4, L-Glu(OMe), of molecules **A** and **B**, which generate a *C*-terminal type-I β-turn, instead of the classical type-III β-turn of a normal 3_{10}-helix. Here too, the *C*-terminal Aib residue is helical but of opposite screw sense.

Despite the similarity in sequence, -(Aib)$_2$-L-Xxx-Aib-, the folding motifs of the two fully protected tetrapeptide esters **4 I** and **4 II** are quite distinct. Formation of two, consecutive, type-III β-turns (although the *C*-terminal β-turn is slightly distorted) in a tetrapeptide such as **4 I** is a common outcome. In contrast, the backbone of **4 II** starts as a type-II′β-turn and is followed by a highly distorted type-I β-turn. This result implies that the Aib residue at position 1 of **4 I** accommodates in the very unusual *semi*-extended (instead of the classical helical) conformation. Again, the *C*-terminal Aib residue of both tetrapeptides is helical but of opposite screw sense.

Both the N$^{\alpha}$-blocked tripeptide ester **3 I** and dipeptide amide **3 III**, although lacking chiral centers, crystallize in noncentrosymmetric space groups. The tripeptide ester **3 I** is folded in a type-III β-turn conformation, whereas the dipeptide amide **3 III** is folded in a β-turn conformation that, on the basis of the backbone torsion angles, can be classified as intermediate between type-III′ and I′. Again, the *C*-terminal Aib residue of the tripeptide is helical but

DOI: 10.1002/psc

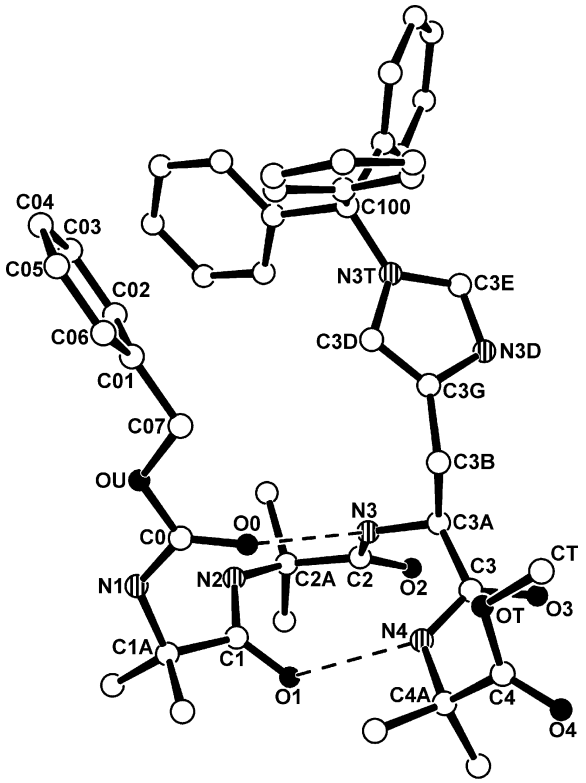

Figure 5 X-ray diffraction structure of Z-(Aib)$_2$-L-His(N$^{\tau}$-Trt)-Aib-OMe (**4 I**) with numbering of the atoms. The two intramolecular H-bonds are represented by dashed lines.

of opposite handedness with respect to the preceding residues.

Conversely, the achiral, N$^{\alpha}$-blocked dipeptide amide **3 II** crystallizes in a centrosymmetric space group, as usual for achiral compounds, in which molecules of both handedness are found. This dipeptide amide is folded in a type-III (III′) β-turn conformation.

The N$^{\alpha}$-phthaloyl dipeptide ester **2 I** was prepared as a racemate [only the torsion angles and the molecular structure of the compound containing the (1*R*, 2*R*) enantiomer of the βAc$_6$c residue are shown in Table 5 and Figure 10, respectively]. Its sequence is based on an α-amino acid followed by a β-amino acid. The Aib ψ_1 torsion angle is indicative of the onset of a helical conformation for this 'imide-type' residue [25,36]. The β-amino acid is partially folded, with the 'ϕ_2', δ (around the central C2B1-C2A bond), and 'ψ_2' torsion angles 144.6(2)°, −58.0(2)°, and −25.7(2)°, respectively [50].

At variance with **2 I** in the achirals N$^{\alpha}$-phthaloyl α-amino amide **2 II** the 'imide-type' Aib residue is extended with 'ψ_1' 175.8(2)°. Conversely, the Aib-based α-aminodialkylperoxide moiety is folded [25]. Again, the torsion angles (Table 5) and molecular structure (Figure 11) of only one enantiomer are reported.

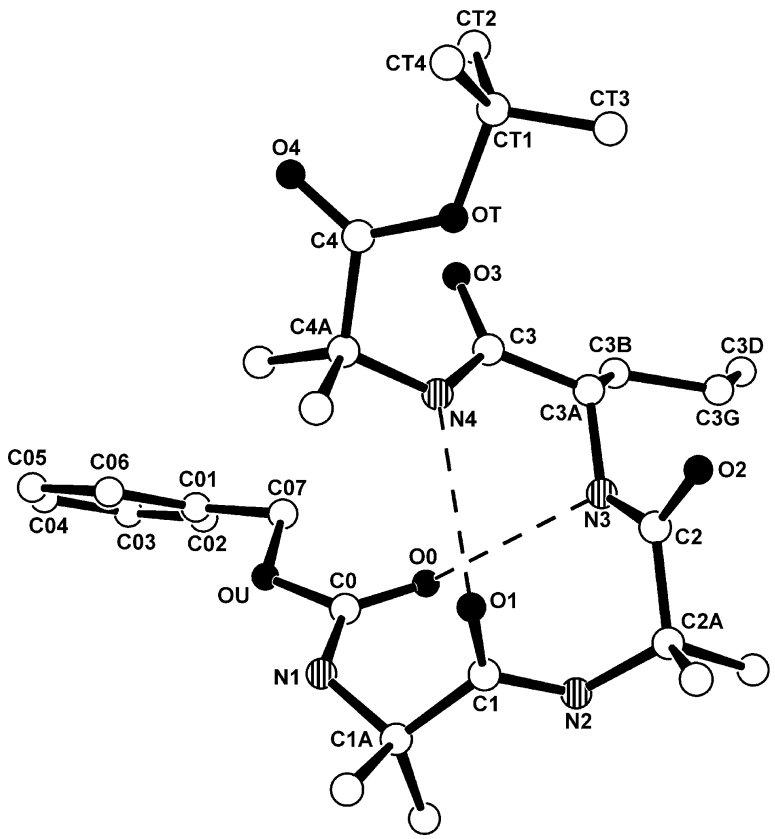

Figure 6 X-ray diffraction structure of Z-(Aib)$_2$-L-Nva-Aib-O*t*Bu (**4 II**) with numbering of the atoms. The two intramolecular H-bonds are represented by dashed lines.

DOI: 10.1002/psc

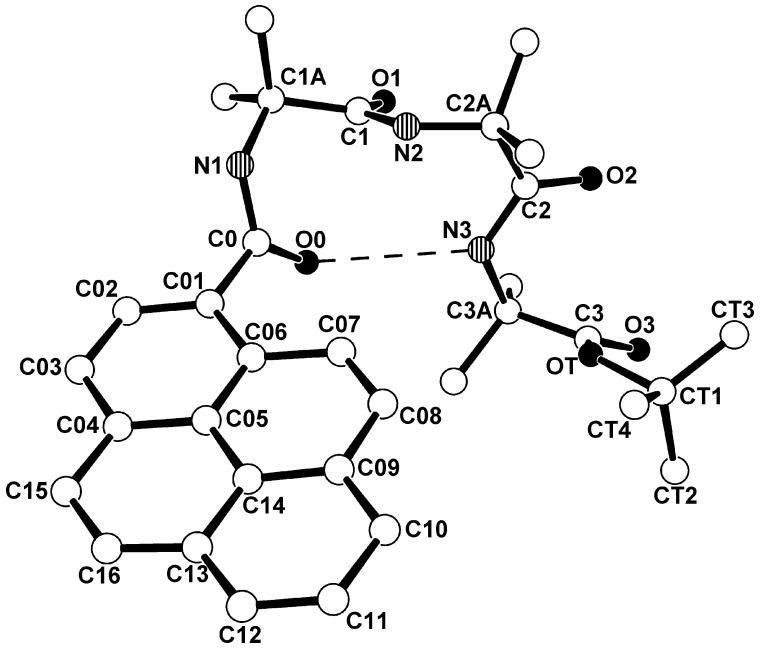

Figure 7 X-ray diffraction structure of Pyr-$(Aib)_3$-O*t*Bu (**3 I**) with numbering of the atoms. The intramolecular H-bond is represented by a dashed line.

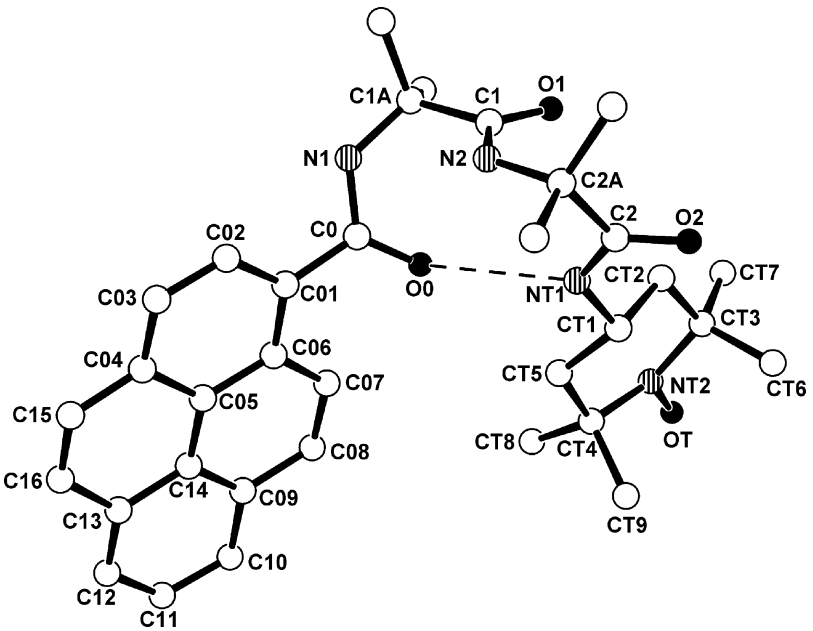

Figure 8 X-ray diffraction structure of Pyr-$(Aib)_2$-(4)NH-TEMPO (**3 II**) with numbering of the atoms. The intramolecular H-bond is represented by a dashed line. Only the right-handed turn structure is shown.

The 3D-structures of the common part of the sequence of the *retro*-peptides [51,52] Boc-*g*Gly-*m*Aib-OH (**2 III**) and $^{+}H_2$-*g*Gly-*m*Aib-O*t*Bu [26] are quite similar, both of them being mostly folded.

The two independent molecules in the asymmetric unit of **6** also differ by the orientation of their L-*a*Ile[1] side chains (g^- g^+ for molecule **A** and t g^- for molecule **B**). In all four independent molecules in the asymmetric unit of **5**, the L-Glu(O*t*Bu)[3] side chains (χ^1 and χ^2 torsion angles) are of the g^-, t type. The χ^1 torsion angle of the L-His(τ-Trt) residue of **4 I** is g^- and the χ^2 torsion angles are *skew*. In **4 II**, the L-Nva χ^1, χ^2 set of torsion angles is g^-, t. Such side-chain dispositions are among those most commonly found for these amino acid residues in peptides [53].

The cyclohexane ring of the βAc_6c residue of **2 I** adopts a chair disposition. The puckering parameters [54] are $Q_T = 0.583(3)$ Å, $\theta_2 = 2.4(3)^\circ$, and $\varphi_2 = 245(6)^\circ$.

DOI: 10.1002/psc

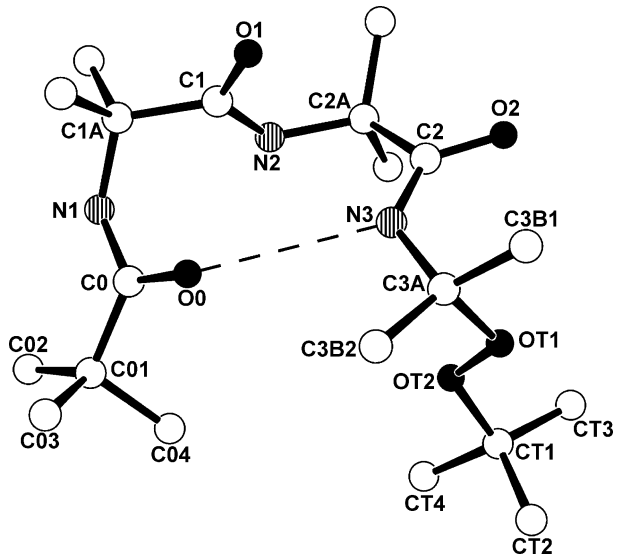

Figure 9 X-ray diffraction structure of Piv-(Aib)$_2$-NH-C(CH$_3$)$_2$-*O*-O*t*Bu (**3 III**) with numbering of the atoms. The intramolecular H-bond is represented by a dashed line.

Both the amino and carboxyl substituents occupy an equatorial position.

All urethane, amide, peptide, and ester groups (ω or χ^4 torsion angles, the latter for the L-Glu γ-ester function) are *trans*, with only ω_6 of **7**, ω_0 and ω_5 (both molecules **A** and **B**) of **6**, ω_1 (molecule **A**) and ω_4 (molecules **B** and **C**) of **5**, ω_1 and ω_3 of **4 I**, ω_0 and ω_3 of **4 II**, ω_1 of **3 I**, ω_0 and ω_2 of **3 III**, and ω_0 and ω_2 of **2 II** deviating substantially ($>10^\circ$) from the 180° planar disposition. The conformation of the six Z-urethane groups (molecules **A**–**D** of **5, 4 I**, and **4 II**) and the single Boc-urethane group (**2 III**), involving the θ^1 and ω_0 torsion angles, is the usual *trans, trans* or type-*b* conformation [34,35]. The piperidine ring of the 4-amino-TEMPO moiety of **3 II** is found in a distorted *chair* ($^4C_1$) disposition, characterized by the following puckering parameters [54] (relative to the atom sequence NT2-CT4-CT5-CT1-CT2-CT3): $Q_T = 0.500(4)$ Å, $\theta_2 = 153.5(4)^\circ$, and $\varphi_2 = 11.1(10)^\circ$ [55].

The packing mode of **7** is characterized by the occurrence of a single, weak, intermolecular H-bond, between the (peptide) N2–H group and the (peptide)

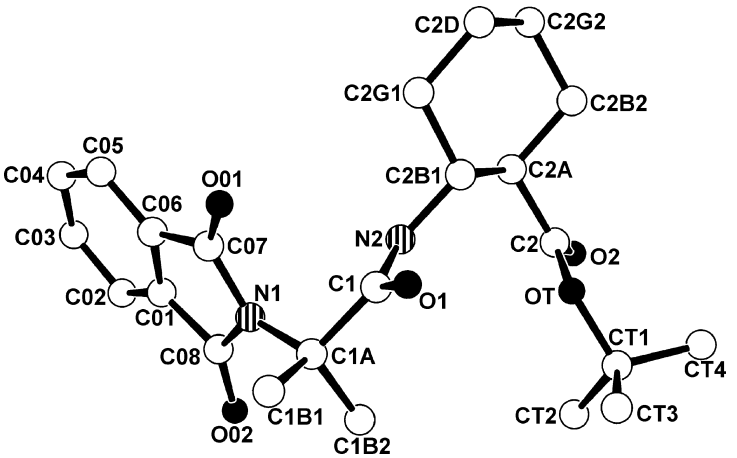

Figure 10 X-ray diffraction structure of Pht-Aib-βAc$_6$c-O*t*Bu (**2 I**) with numbering of the atoms. Only the dipeptide from the (1*R*, 2*R*) enantiomer is shown.

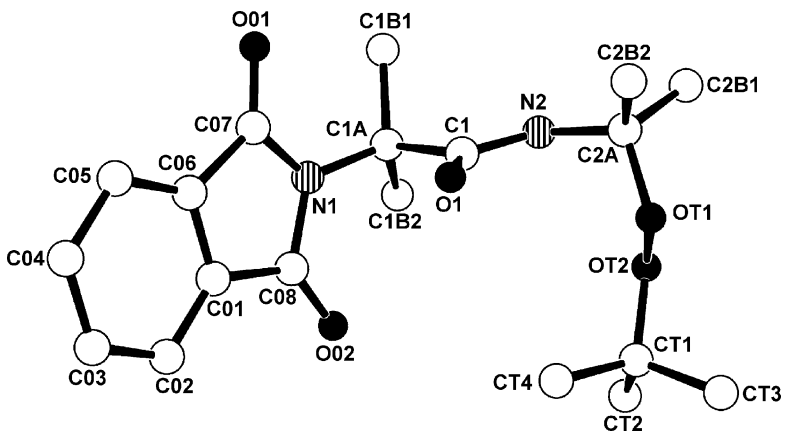

Figure 11 X-ray diffraction structure of Pht-Aib-NH-C(CH$_3$)$_2$-*O*-O*t*Bu (**2 II**) with numbering of the atoms. Only one of the two enantiomeric forms is shown.

DOI: 10.1002/psc

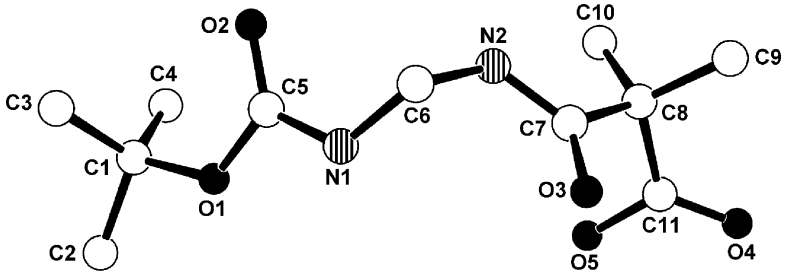

Figure 12 X-ray diffraction structure of Boc-*g*Gly-*m*Aib-OH (**2 III**) with numbering of the atoms. Only one of the two enantiomeric forms is shown.

Table 4 N^{α}-Blocking Group and Backbone Torsion Angles (°) for the Longest Five Peptides Studied in this Work

Torsion angle	**7**	**6**		**5**				**4 I**	**4 II**
		Mol. **A**	Mol. **B**	Mol. **A**	Mol. **B**	Mol. **C**	Mol. **D**		
θ^2	—	—	—	74.0(17)	74.5(16)	72.8(16)	73.4(16)	168.5(5)	165.4(3)
θ^1	—	—	—	−174.9(13)	−168.8(13)	−166.4(13)	−171.1(13)	176.4(5)	−178.1(3)
ω_0	172.3(3)[a]/−171.6(4)[b]	166.6(4)	−165.7(4)	180.0(13)	−173.6(12)	−176.0(12)	−172.1(12)	175.8(4)	166.5(3)
ϕ_1	45.7(5)[c]/−150.1(4)[d]	42.4(5)	−63.8(5)	−53.1(19)	−57.2(19)	−57.6(17)	−60.1(17)	−50.8(6)	53.7(4)
ψ_1	−132.2(3)	57.0(4)	−41.1(5)	−42.2(19)	−31.3(19)	−32.8(17)	−32.2(17)	−42.0(6)	−123.1(3)
ω_1	−162.7(3)	172.2(3)	−176.6(4)	−168.6(13)	−172.0(12)	−175.0(11)	−172.8(11)	−167.6(5)	−171.8(3)
ϕ_2	−53.7(4)	52.6(5)	−51.5(6)	−56(2)	−60.3(18)	−56.2(17)	−59.5(17)	−59.5(7)	−54.8(4)
ψ_2	−30.9(4)	34.7(5)	−34.8(5)	−25.6(19)	−26.2(17)	−28.1(18)	−28.1(17)	−30.3(6)	−36.4(4)
ω_2	−178.6(3)	174.0(3)	−174.5(3)	−179.4(11)	179.6(11)	177.9(12)	−177.4(12)	180.0(4)	−175.3(3)
ϕ_3	−52.6(4)	52.4(4)	−53.5(5)	−53.3(17)	−55.5(16)	−53.1(18)	−55.4(17)	−86.0(6)	−102.5(4)
ψ_3	−31.6(4)	36.4(5)	−36.1(5)	−32.7(16)	−31.3(17)	−24.0(18)	−27.9(17)	−26.1(7)	25.5(5)
ω_3	−178.8(3)	172.1(3)	−174.3(3)	−176.5(11)	−173.2(11)	178.5(12)	−177.2(12)	−167.1(5)	169.7(3)
ϕ_4	−52.5(4)	57.2(5)	−54.7(5)	−75.5(17)	−80.5(16)	−68.7(18)	−61.1(18)	39.3(7)	−50.4(4)
ψ_4	−32.2(4)	35.8(5)	−37.0(5)	−11.5(19)	−3.1(18)	−24.0(19)	−32(2)	46.6(6)[q]	−34.5(4)[q]
ω_4	−173.6(3)	175.6(3)	−174.8(3)	−175.1(13)	−169.4(11)	169.9(12)	175.0(12)	−176.5(5)[r]	173.7(3)[r]
ϕ_5	−56.0(5)	65.7(5)	−62.8(5)	52.0(18)	47.0(17)	45.8(17)	49.7(17)	—	—
ψ_5	−30.0(5)	34.3(4)	−36.0(5)	31.6(19)[i]	43(2)[j]	53.8(15)[k]	51.3(16)[l]	—	—
ω_5	−173.7(4)	164.4(3)	−164.7(4)	178.7(15)[m]	171.5(18)[n]	−178.7(12)[o]	178.1(13)[p]	—	—
ϕ_6	−68.3(5)	−47.1(5)	48.2(5)	—	—	—	—	—	—
ψ_6	−18.4(5)	−45.2(4)[e]	45.4(5)[f]	—	—	—	—	—	—
ω_6	−167.8(3)	−175.0(4)[g]	174.2(4)[h]	—	—	—	—	—	

[a] C01-C08-N1-C1A.
[b] C06-C07-N1-C1A.
[c] C08-N1-C1A-C1.
[d] C07-N1-C1A-C1.
[e] N6-C6A-C6-OTA.
[f] N12-C12A-C12-OTB.
[g] C6A-C6-OTA-CT1A.
[h] C12A-C12-OTB-CT1B.
[i] N5-C5A-C5-OTA.
[j] N15-C15A-C15-OTB.
[k] N25-C25A-C25-OTC.
[l] N35-C35A-C35-OTD.
[m] C5A-C5-OTA-CT1A.
[n] C15A-C15-OTB-CT1B.
[o] C25A-C25-OTC-CT1C.
[p] C35A-C35-OTD-CT1D.
[q] N4-C4A-C4-OT.
[r] C4A-C4-OT-CT.

DOI: 10.1002/psc

Table 5 N^{α}-Blocking Group and Backbone Torsion Angles (°) for the Additional Six Peptides Studied in this Work

Torsion angle	**3 I**	**3 II**	**3 III**	**2 I** [(1*R*, 2*R*) enantiomer]	**2 II**	**2 III**
θ^2	—	—	—	—	—	—
θ^1	—	—	—	—	—	179.8(2)
ω_0	−172.0(6)	−179.1(3)	167.1(6)	−176.7(1)[c]/177.6(2)[d]	−167.6(2)[c]/168.9(2)[d]	175.4(2)
ϕ_1	−43.2(9)	−48.1(4)	51.2(8)	−51.4(2)[e]/137.9(2)[f]	88.7(2)[e]/−70.0(2)[f]	−90.3(2)[m]
ψ_1	−50.2(8)	−37.7(3)	45.1(8)	−44.0(2)	175.8(1)	−89.6(7)[n]
ω_1	−169.0(6)	−178.3(2)	170.2(6)	−179.9(2)	176.8(2)	177.0(2)[o]
ϕ_2	−60.0(9)	−54.1(3)	69.9(8)	144.6(2)[g]	68.5(2)[j]	−135.9(2)[o]
ψ_2	−27.9(9)	−28.8(4)	13.6(8)	−25.7(2)[h]	58.0(2)[k]	57.2(2)[q]
ω_2	−173.2(6)	177.1(2)	164.7(6)	−177.6(1)[i]	−156.5(1)[l]	
ϕ_3	53.8(9)	—	—	—	—	—
ψ_3	46.9(8)[a]	—	—	—	—	—
ω_3	173.5(6)[b]	—	—	—	—	

[a] N3-C3A-C3-OT.
[b] C3A-C3-OT-CT1.
[c] C06-C07-N1-C1A.
[d] C01-C08-N1-C1A.
[e] C07-N1-C1A-C1.
[f] C08-N1-C1A-C1.
[g] C1-N2-C2B1-C2A.
[h] C2B1-C2A-C2-OT.
[i] C2A-C2-OT-CT1.
[j] C1-N2-C2A-OT1.
[k] N2-C2A-OT1-OT2.
[l] C2A-OT1-OT2-CT1.
[m] C5-N1-C6-N2.
[n] N1-C6-N2-C7.
[o] C6-N2-C7-C8.
[p] N2-C7-C8-C11.
[q] C7-C8-C11-O5.

O5=C5 group of a $(5/2 - x, 1/2 + y, 1/2 + z)$ symmetry related molecule (Table 6), giving rise to rows of molecules, head-to-tail H-bonded, in a zig-zag motif along the *a* direction.

In the unit cell of **6**, molecules **A** and **B**, chosen as the asymmetric unit, lay antiparallel, both with the helix axis along the *b* direction. Molecule **A** is head-to-tail H-bonded to its own $(x, 1 + y, z)$ translational equivalent, through N1···O4 and N2···O5 N–H···O=C H-bonds. Similarly, the intermolecular H-bonds formed by the N7 and N8 N–H groups of molecule **B** have the O10 and O11 carbonyl oxygen atoms as the acceptors, respectively, of a $(x, -1 + y, z)$ translational equivalent of molecule **B**. Thus, rows of molecules of the same kind are observed along the *b* direction.

In the packing mode of **5**, each of the four independent peptide molecules is intermolecularly H-bonded to its own translational equivalents, giving rise to rows of molecules of the same kind along the *a* direction. Specifically, the H-bonds connect the *N*-terminal N–H group to the C=O group of the penultimate residue of either a $(x + 1, y, z)$ translational equivalent (molecules **A** and **C**), or a $(x\text{-}1, y, z)$ translational equivalent (molecules **B** and **D**). The N–H group of the second residue of all four independent molecules does not participate in the intermolecular H-bonding scheme.

Two types of intermolecular H-bonds are found in the packing mode of **4 I**, one connecting the N1–H group to the (imidazole) N3D atom of a $(x, y, z + 1)$ symmetry related molecule, and the other between the N2–H group and the O4 carbonyl oxygen atom of a $(x + 1, y, z + 1)$ symmetry related molecule. These two interactions link molecules along the *C* and the *ac* directions, respectively.

In the packing mode of **4 II**, an intermolecular H-bond between the N1–H group and the O3=C3 group (symmetry equivalence: $-x, -1/2 + y, 1/2 - z$) generates rows of molecules related by a two-fold screw axis along the *b* direction. A second H-bond, namely, N2–H···O2=C2 (symmetry equivalence: $-1/2 + x, 1/2 - y, -z$) links molecules, again related by a two-fold screw axis, along the *a* direction.

A single type of intermolecular H-bond characterizes the packing mode of **3 I**, between the N1–H group and the O1=C1 group of a $(1 - x, -1/2 + y, 1 - z)$ symmetry related molecule, connecting molecules related by the two-fold screw axis along the *b* direction. The N2–H

DOI: 10.1002/psc

Table 6 Intra and Intermolecular H-Bond Parameters for the Eleven Peptides Studied in this Work

Peptide	Type	Donor D–H	Acceptor A	Distance (Å) D···A	Distance (Å) H···A	Angle (°) D–H···A	Symmetry operation of A
7	Intramolecular	N3-H	O02	3.253(4)	2.52	143	x, y, z
		N4-H	O1	2.948(3)	2.12	163	x, y, z
		N5-H	O2	2.938(4)	2.11	162	x, y, z
		N6-H	O3	3.146(4)	2.31	164	x, y, z
		N7-H	O4	3.133(4)	2.30	164	x, y, z
	Intermolecular	N2-H	O5	3.075(4)	2.54	121	$5/2 - x, 1/2 + y, 1/2 + z$
6	Intramolecular	N3-H	O0A	2.953(4)	2.20	146	x, y, z
		N4-H	O1	3.053(4)	2.24	157	x, y, z
		N5-H	O2	3.104(4)	2.35	147	x, y, z
		N6-H	O3	3.101(5)	2.32	151	x, y, z
		N9-H	O0B	3.187(5)	2.45	145	x, y, z
		N10-H	O7	2.958(4)	2.17	153	x, y, z
		N11-H	O8	3.096(4)	2.33	149	x, y, z
		N12-H	O9	3.069(5)	2.29	150	x, y, z
	Intermolecular	N1-H	O4	2.832(4)	1.98	174	$x, 1 + y, z$
		N2-H	O5	3.152(4)	2.36	154	$x, 1 + y, z$
		N7-H	O10	2.886(4)	2.04	170	$x, -1 + y, z$
		N8-H	O11	3.232(4)	2.44	154	$x, -1 + y, z$
5	Intramolecular	N3-H	O0A	3.127(13)	2.31	159	x, y, z
		N4-H	O1	3.029(13)	2.20	161	x, y, z
		N5-H	O2	3.025(15)	2.18	169	x, y, z
		N13-H	O0B	3.052(13)	2.23	161	x, y, z
		N14-H	O11	2.982(13)	2.16	161	x, y, z
		N15-H	O12	3.112(15)	2.29	160	x, y, z
		N23-H	O0C	3.087(14)	2.27	158	x, y, z
		N24-H	O21	2.979(12)	2.13	170	x, y, z
		N25-H	O22	3.038(14)	2.28	148	x, y, z
		N33-H	O0D	3.189(14)	2.38	157	x, y, z
		N34-H	O31	3.010(14)	2.17	166	x, y, z
		N35-H	O32	2.981(13)	2.22	148	x, y, z
	Intermolecular	N1-H	O4	2.849(13)	2.00	167	$1 + x, y, z$
		N11-H	O14	2.895(13)	2.04	176	$-1 + x, y, z$
		N21-H	O24	2.788(13)	2.02	149	$1 + x, y, z$
		N31-H	O34	2.795(14)	2.04	147	$-1 + x, y, z$
4 I	Intramolecular	N3-H	O0	3.161(7)	2.40	148	x, y, z
		N4-H	O1	3.005(6)	2.25	147	x, y, z
	Intermolecular	N1-H	N3D	3.267(8)	2.44	162	$x, y, 1 + z$
		N2-H	O4	2.832(6)	2.14	137	$1 + x, y, 1 + z$
4 II	Intramolecular	N3-H	O0	2.974(4)	2.27	139	x, y, z
		N4-H	O1	2.992(3)	2.16	164	x, y, z
	Intermolecular	N1-H	O3	2.871(3)	2.28	126	$-x, -1/2 + y, 1/2 - z$
		N2-H	O2	3.124(3)	2.30	160	$-1/2 + x, 1/2 - y, -z$
3 I	Intramolecular	N3-H	O0	3.018(8)	2.20	158	x, y, z
	Intermolecular	N1-H	O1	3.005(7)	2.32	137	$1 - x, -1/2 + y, 1 - z$
3 II	Intramolecular	NT1-H	O0	2.864(3)	2.06	155	x, y, z
	Intermolecular	N1-H	O2	2.880(3)	2.17	139	$1 + x, y, z$
		N2-H	OT	3.107(4)	2.43	136	$1 + x, 1 + y, z$
3 III	Intramolecular	N3-H	O0	3.067(7)	2.23	165	x, y, z
	Intermolecular	N1-H	O1	3.233(7)	2.79	114	$-1/2 - x, -1/2 + y, 2 - z$
2 I	Intermolecular	N2-H	O2	2.988(2)	2.15	166	$1 - x, -y, 1 - z$
2 II	Intermolecular	N2-H	O01	3.297(2)	2.45	170	$-1/2 + x, 1 - y, z$
2 III	Intermolecular	N1-H	O2	2.911(2)	2.08	166	$1/2 + x, 1/2 - y, z$
		N2-H	O3	2.999(2)	2.17	161	$-1/2 + x, 1/2 - y, z$
		O5-H	O4	2.625(2)	1.81	175	$2 - x, 1 - y, 1 - z$

DOI: 10.1002/psc

group does not participate in the intermolecular H-bonding scheme.

In the packing mode of **3 II**, the N1–H group is H-bonded to the O2 carbonyl oxygen atom of a $(1+x, y, z)$ symmetry related molecule, generating rows of molecules along the *a* direction. A second H-bond is observed between the N1–H group and the (nitroxide) OT atom (symmetry equivalence: $1+x, 1+y, z$). This latter interaction connects molecules along the *ab* direction. In addition, significant π stacking is found between the pyrene aromatic ring and its $(1-x, -y, -z)$ symmetry equivalent. This centrosymmetric arrangement determines a full overlapping of the rings, bringing the C01 atom of one molecule close to the C12 atom of the other, C07 to C16, C11 to C02, and so on, with distances ranging from 3.69 to 3.74 Å. On the opposite face of the (x, y, z) pyrene ring, an additional $(2-x, -y, -z)$ symmetry equivalent is located. In this latter case, however, the two rings approach only through their apical C13, C15 and C16 atoms, at distances C16···C16, C13···C15, and C15···C13 of 3.33, 3.80 and 3.80 Å, respectively.

In the packing mode of **3 III**, the only intermolecular, relatively short, N–H···O=C distance [3.233(7) Å] is observed between the N1–H group and the O1 carbonyl oxygen atom (symmetry equivalence $-1/2-x, -1/2+y, 2-z$). However, the corresponding H···O distance and the N–H···O angle (reported in Table 6) are outside the generally accepted limits for the occurrence of N–H···O H-bonds. Interestingly, the N1–H group is to some extent shielded by the methyl groups C02 and C1B2 of the pivaloyl group and the Aib(1) residue, respectively. Indeed, these latter two methyl groups make short C–H···O intermolecular contacts with the O1 atom mentioned above, with C···O distances between 3.53 and 3.58 Å. These contacts connect molecules related by a two-fold screw axis along the *b* direction.

The packing mode of **2 I** is characterized by the occurrence of centrosymmetric dimers, held together by (peptide) N2–H···O2=C2 (ester) (symmetry equivalence $1-x, -y, 1-z$) intermolecular H-bonds.

In the packing mode of **2 II**, the molecules are connected by an N2–H···O01=C07 (symmetry equivalence $-1/2+x, 1-y, z$) intermolecular H-bond, thus generating a zig-zag motif along the *a* direction.

In the packing mode of **2 III**, each molecule is connected on one side to its $1/2+x, 1/2-y, z$ symmetry equivalent through an N1–H···O2=C5 H-bond, and on the other side to its $-1/2+x, 1/2-y, z$ symmetry equivalent through an N2–H···O3=C7 H-bond, thus generating rows of molecules of the same handedness along the *a* direction. In addition, each molecule is linked to its $2-x, 1-y, 1-z$ centrosymmetric counterpart by formation of a carboxylic acid···carboxylic acid dimer stabilized by O5–H···O4=C11 intermolecular H-bonds.

CONCLUSIONS

The homo-oligopeptide dialkyl peroxides **7**, **3 III**, and **2 II** were serendipitously synthesized [25] during our attempted preparation of the corresponding peroxyesters [56]. In the same framework, the dipeptide ester **2 I** is a synthetic precursor of the related peroxyester [56]. The hexapeptide **6** is an additional example of our synthetic and conformational work aimed at understanding the relationship between *N*-terminal α-amino acid α-carbon chirality and helical screw sense of the peptide molecule [49,57,58]. Peptides **5, 3 I**, and **3 II**, containing either the naphthyl or the pyrenyl fluorophore, were prepared in our continuing study of molecular spacers for physicochemical investigations based on turn/helical peptide structures [21]. The tetrapeptide **4 I** is a synthetic intermediate for the construction of a catalytically active peptide template [59]. The tetrapeptide **4 II** was prepared for a comparative conformational study with the corresponding peptide containing a residue of C^{α}-methyl norvaline [60]. Boc-*g*Gly-*m*Aib-OH (**2 III**) is a starting building block for the synthesis of an oligomeric series of sequential *retro*-peptide foldamers [26].

In this X-ray diffraction work it was found that all Aib residues (except two) are folded, with sets of ϕ,ψ torsion angles falling in the helical regions A/A* of the Ramachandran map [61]. The only two exceptions refer to the *semi*-extended residue 1 of both the hexapeptide amide **7** and the tetrapeptide **4 II**. All potentially donor N–H groups from position 3 in the sequences to the *C*-terminal residue, or even to the *C*-terminal amide group whenever present (peptides **7, 3 II**, and **3 III**), form intramolecular H-bonds, thus originating the maximum number of consecutive β-turns compatible with the main-chain length. The present study also confirms that a helical peptide molecule characterized by a single chiral residue at the *N*-terminus (e.g. hexapeptide **6**) may produce a crystal containing two diastereomeric compounds [49]. This phenomenon has also been found when the single chiral residue is positioned either in an internal position of the sequence or at its *C*-terminus [57,58,62].

Acknowledgements

The authors are grateful to Prof. Claudia Tomasini, Department of Chemistry 'G. Ciamician', University of Bologna, Italy, for kindly providing a sample of Boc-*g*Gly-*m*Aib-OH.

REFERENCES

1. Karle IL, Balaram P. Structural characteristics of α-helical peptide molecules containing Aib residues. *Biochemistry* 1990; **29**: 6747–6756.

2. Toniolo C, Benedetti E. Structures of polypeptides from α-amino acids disubstituted at the α-carbon. *Macromolecules* 1991; **24**: 4004–4009.
3. Toniolo C, Crisma M, Formaggio F, Valle G, Cavicchioni G, Précigoux G, Aubry A, Kamphuis J. Structures of peptides from α-amino acids methylated at the α-carbon. *Biopolymers* 1993; **33**: 1061–1072.
4. Toniolo C, Crisma M, Formaggio F, Peggion C. Control of peptide conformation by the Thorpe-Ingold effect (C^{α}-tetrasubstitution). *Biopolymers (Pept. Sci.)* 2001; **60**: 396–419.
5. Marshall GR. In *Intra-Science Chemistry Reports*, Vol. 5, Kharasch N (ed.). Gordon and Breach: New York, 1971; 305–316.
6. Burgess AW, Leach SJ. An obligatory α-helical amino acid residue. *Biopolymers* 1973; **12**: 2599–2605.
7. Venkataram Prasad BV, Sasisekharan V. A case study of the conformation of poly(α-aminoisobutyric acid): α- or 3_{10}-helix. *Macromolecules* 1979; **12**: 1107–1110.
8. Paterson Y, Rumsey SM, Benedetti E, Némethy G, Scheraga HA. Sensitivity of peptide conformation to geometry. Theoretical conformational analysis of oligomers of α-aminoisobutyric acid. *J. Am. Chem. Soc.* 1981; **103**: 2947–2955.
9. Venkatachalam CM. Stereochemical criteria for polypeptides and proteins. V. Conformation of a system of three-linked peptide units. *Biopolymers* 1968; **6**: 1425–1436.
10. Toniolo C. Intramolecularly hydrogen-bonded peptide conformations. *CRC Crit. Rev. Biochem.* 1980; **9**: 1–44.
11. Rose GD, Gierasch LM, Smith PJ. Turns in peptides and proteins. *Adv. Protein Chem.* 1985; **37**: 1–109.
12. Barlow DJ, Thornton JM. Helix geometry in proteins. *J. Mol. Biol.* 1988; **201**: 601–619.
13. Toniolo C, Benedetti E. The polypeptide 3_{10}-helix. *Trends Biochem. Sci.* 1991; **16**: 350–353.
14. Karpen ME, de Haseth PL, Neet KE. Differences in the amino acid distributions of 3_{10}-helices and α-helices. *Protein Sci.* 1992; **1**: 1333–1342.
15. Bolin KA, Millhauser GL. The split personality of polypeptide helices. *Acc. Chem. Res.* 1999; **32**: 1027–1033.
16. Pal L, Basu G. Novel protein structural motifs containing two-turn and longer 3_{10}-helices. *Protein Eng.* 1999; **12**: 811–814.
17. Pal L, Basu G, Chakrabarti P. Variants of 3_{10}-helices in proteins. *Proteins: Struct. Funct. Genet.* 2002; **48**: 571–579.
18. Pal L, Chakrabarti P, Basu G. Sequence and structure patterns in proteins from an analysis of the shortest helices: implications for helix nucleation. *J. Mol. Biol.* 2003; **326**: 273–291.
19. Némethy G, Printz MP. The γ-turn, a possible folded conformation of the polypeptide chain. Comparison with the β-turn. *Macromolecules* 1972; **5**: 755–758.
20. Cung MT, Marraud M, Néel J. Étude expérimentale de la conformation des molécules dipeptidiques. Comparison avec les prévisions théoriques. *Ann. Chim. (Paris)* 1972; **7**: 183–209.
21. Toniolo C, Crisma M, Formaggio F, Peggion C, Broxterman QB, Kaptein B. Molecular spacers for physicochemical investigations based on novel helical and extended peptide structures. *Biopolymers (Pept. Sci.)* 2004; **76**: 162–176.
22. Moretto V, Crisma M, Bonora GM, Toniolo C, Balaram H, Balaram P. Comparison of the effect of five guest residues on the β-sheet conformation of host $(L\text{-}Val)_n$ oligopeptides. *Macromolecules* 1989; **22**: 2939–2944.
23. Formaggio F, Bettio A, Moretto V, Crisma M, Toniolo C, Broxterman QB. Disruption of the β-sheet structure of a protected pentapeptide, related to the β-amyloid sequence 17–21, induced by a single, helicogenic, C^{α}-tetrasubstituted α-amino acid. *J. Pept. Sci.* 2003; **9**: 461–466.
24. Gilead S, Gazit E. Inhibition of amyloid formation by peptide analogues modified with α-aminoisobutyric acid. *Angew. Chem., Int. Ed. Engl.* 2004; **43**: 4041–4044.
25. Moretto A, De Zotti M, Scipionato L, Formaggio F, Crisma M, Toniolo C, Antonello S, Maran F, Broxterman QB. Serendipitous discovery of peptide dialkyl peroxides. *Helv. Chim. Acta* 2002; **85**: 3099–3112.
26. Ceretti S, Luppi G, De Pol S, Formaggio F, Crisma M, Toniolo C, Tomasini C. Total synthesis of sequential retro-peptide oligomers. *Eur. J. Org. Chem.* 2004; 4188–4196.
27. Sheldrick GM. SHELXS 86. *Program for Crystal Structure Determination*. University of Göttingen: Göttingen, 1986.
28. Sheldrick GM. SHELXS 97. *Program for Crystal Structure Determination*. University of Göttingen: Göttingen, 1997.
29. Burla MC, Carrozzini B, Cascarano GL, Giacovazzo C, Polidori G. More power for direct methods: SIR2002. *Z. Kristallogr.* 2002; **217**: 629–635.
30. Sheldrick GM. SHELXL 93. *Program for Crystal Structure Refinement*. University of Göttingen: Göttingen, 1993.
31. Sheldrick GM. SHELXL 97. *Program for Crystal Structure Refinement*. University of Göttingen: Göttingen, 1997.
32. Allen FH. The Cambridge Structural Database: a quarter of a million crystal structures and rising. *Acta Crystallogr.* 2002; **B58**: 380–388.
33. IUPAC-IUB Commission on Biochemical Nomenclature. Abbreviations and symbols for the description of the conformation of polypeptide chains. *Biochemistry* 1970; **9**: 3471–3479.
34. Benedetti E, Pedone C, Toniolo C, Dudek M, Némethy G, Scheraga HA. Preferred conformation of the benzyloxycarbonylamino group in peptides. *Int. J. Pept. Protein Res.* 1983; **21**: 163–181.
35. Benedetti E, Pedone C, Toniolo C, Némethy G, Pottle MS, Scheraga HA. Preferred conformation of the *tert*-butoxycarbonylamino group in peptides. *Int. J. Pept. Protein Res.* 1980; **16**: 156–172.
36. Valle G, Toniolo C, Jung G. Activated amino acids. Structures of [αmacrosdollar-(phthalimido)isobutyric] anhydride, pentachlorophenyl αmacrosdollar-(*tert*-butyloxycarbonylamino) isobutanoate, and pentachlorophenyl αmacrosdollar-(benzyloxycarbonylamino) isobutanoate. *Liebigs Ann. Chem.* 1986; 1809–1822.
37. Aubry A, Cung MT, Marraud M. βI- and βII-turn conformations in model dipeptides with the Pro-Xaa sequences. *J. Am. Chem. Soc.* 1985; **107**: 7640–7647.
38. Valle G, Crisma M, Toniolo C. Structure of N-pivaloyl-N′-methyl-L-prolinamide. *Acta Crystallogr.* 1988; **C44**: 850–853.
39. Chakrabarti P, Dunitz JD. Structural characteristics of the carboxylic amide group. *Helv. Chim. Acta* 1982; **65**: 1555–1562.
40. Schweizer WB, Dunitz JD. Structural characteristics of the carboxylic ester group. *Helv. Chim. Acta* 1982; **65**: 1547–1554.
41. Benedetti E. In *Chemistry and Biochemistry of Amino Acids, Peptides and Proteins.*, Vol. 6, Weinstein B (ed.). Dekker: New York, 1982; 105–184.
42. Ashida T, Tsunogae Y, Tanaka I, Yamane T. Peptide chain structure parameters, bond angles and conformational angles from the Cambridge structural database. *Acta Crystallogr.* 1987; **B43**: 212–218.
43. Paterson Y, Rumsey SM, Benedetti E, Némethy G, Scheraga HA. Sensitivity of polypeptide conformation to geometry. Theoretical conformational analysis of oligomers of α-aminoisobutyric acid. *Int. J. Pept. Protein Res.* 1982; **20**: 468–480.
44. Bosch R, Jung G, Winter W. Structure of the 3_{10}-helical pentapeptide Boc-Aib-L-Ala-Aib-L-Ala-Aib-OMe dihydrate, $C_{24}H_{43}N_5O_8 \cdot 2H_2O$. *Acta Crystallogr.* 1983; **C39**: 776–778.
45. Valle G, Crisma M, Formaggio F, Toniolo C, Jung G. Geometry and conformation of the α-aminoisobutyric acid residue in simple derivatives and dipeptides. Four new x-ray structural analyses and a statistical analysis from known crystal data. *Liebigs Ann. Chem.* 1987; 1055–1060.
46. Ramakrishnan C, Prasad N. Study of hydrogen bonds in amino acids and peptides. *Int. J. Pept. Protein Res.* 1971; **3**: 209–231.
47. Taylor R, Kennard O, Versichel W. The geometry of the N–H···O=C hydrogen bond. 3. Hydrogen-bond distances and angles. *Acta Crystallogr.* 1984; **B40**: 280–288.
48. Görbitz CH. Hydrogen-bond distances and angles in the structures of amino acids and peptides. *Acta Crystallogr.* 1989; **B45**: 390–395.

DOI: 10.1002/psc

49. Benedetti S, Saviano M, Iacovino R, Crisma M, Formaggio F, Toniolo C. Helical screw sense of peptide molecules. Crystal structures of three Aib-based pentapeptides. *Z. Kristallogr.* 1999; **214**: 160–166.
50. Cheng RP, Gellman SH, DeGrado WF. β-Peptides: from structure to function. *Chem. Rev.* 2001; **101**: 3219–3232.
51. Goodman M, Chorev M. On the concept of linear modified retro-peptide structures. *Acc. Chem. Res.* 1979; **12**: 1–7.
52. Chorev M, Goodman M. A dozen years of retro-inverso peptidomimetics. *Acc. Chem. Res.* 1993; **26**: 266–273.
53. Benedetti E, Morelli G, Némethy G, Scheraga HA. Statistical and energetic analysis of side-chain conformations in oligopeptides. *Int. J. Pept. Protein Res.* 1983; **22**: 1–15.
54. Cremer D, Pople JA. A general definition of ring puckering coordinates. *J. Am. Chem. Soc.* 1975; **97**: 1354–1358.
55. Crisma M, Deschamps JR, George C, Flippen-Anderson JL, Kaptein B, Broxterman QB, Moretto A, Oancea S, Jost M, Formaggio F, Toniolo C. A topographically and conformationally constrained, spin-labeled, α-amino acid: crystallographic characterization in peptides. *J. Pept. Res.* 2005; **65**: 564–579.
56. Formaggio F, Crisma M, Scipionato L, Antonello S, Maran F, Toniolo C. Synthesis and characterization of a series of homo-oligoperoxyesters. *Org. Lett.* 2004; **6**: 2753–2756.
57. Benedetti E, Saviano M, Iacovino R, Pedone C, Santini A, Crisma M, Formaggio F, Toniolo C, Broxterman QB, Kamphuis J. Helical screw sense of peptide molecules: the pentapeptide system $(Aib)_4$/L-Val [L-(αMe)Val] in the crystal state. *Biopolymers* 1998; **46**: 433–443.
58. Pengo B, Formaggio F, Crisma M, Toniolo C, Bonora GM, Broxterman QB, Kamphuis J, Saviano M, Iacovino R, Rossi F, Benedetti E. Linear oligopeptides. Part 406. Helical screw sense of peptide molecules: the pentapeptide system $(Aib)_4$/L-Val [L-(αMe)Val] in solution. *J. Chem. Soc., Perkin Trans. 2* 1998; 1651–1657.
59. Toniolo C, Crisma M, Formaggio F, Peggion C, Broxterman QB, Kaptein B. Peptide β-bend and 3_{10}-helix: from 3D-structural studies to applications as templates. *J. Inclusion Phenom. Macrocyclic Chem.* 2005; **51**: 121–136.
60. Moretto A, Peggion C, Formaggio F, Crisma M, Toniolo C, Piazza C, Kaptein B, Broxterman QB, Ruiz I, Diaz-de-Villegas MD, Galvez JA, Cativiela C. (αMe)Nva: stereoselective syntheses and preferred conformations of selected model peptides. *J. Pept. Res.* 2000; **56**: 283–297.
61. Zimmerman SS, Pottle MS, Némethy G, Scheraga HA. Conformational analysis of the 20 naturally occurring amino acid residues using ECEPP. *Macromolecules* 1977; **10**: 1–9.
62. Valle G, Crisma M, Toniolo C, Beisswenger R, Rieker A, Jung G. First observation of a helical peptide containing a chiral residue without a preferred screw sense. *J. Am. Chem. Soc.* 1989; **111**: 6828–6833.

DOI: 10.1002/psc